Solid Freeform Fabrication 2019: Proceedings of the 30th Annual International
Solid Freeform Fabrication Symposium – An Additive Manufacturing Conference
Reviewed Paper

SURFACE ROUGHNESS CHARACTERIZATION IN LASER POWDER BED FUSION ADDITIVE MANUFACTURING

Wesley Eidt, Eric-Paul Tatman, Josiah McCarther, Jared Kastner, Sean Gunther, and Joy Gockel

Department of Mechanical and Materials Engineering, Wright State University, Dayton, Ohio 45435

Abstract

Rough surfaces are known to be a detriment to the fatigue performance of metallic materials, and laser powder bed fusion additive manufacturing (AM) is known to produce surfaces with high roughness. Prior work has shown the relationship between surface roughness metrics and the fatigue performance of AM metals through extensive characterization. This work investigates the influence of processing parameters on the surface roughness for vertical surfaces and surfaces at a downward facing angle. It is not always feasible to characterize the entire specimen, so a representation of the surface variation is also presented. Understanding the surface roughness features through characterization and experimental testing will give insight to help optimize processing parameters for improved AM fatigue performance and build tolerances.

Introduction

Additive Manufacturing (AM) enables the construction of parts with greater complexity than traditional manufacturing processes allow. By building layer-by-layer from the ground up, internal geometrical features become much easier to produce. However, surface roughness is inherent to the AM process. While flat external faces can be polished using grinding or sanding techniques, this is not always possible for internal or curved external surfaces. The presence of surface roughness means that there are numerous sites prime for crack initiation, and this has been shown to significantly decrease fatigue life [1]. Since roughness cannot always be entirely corrected, it is in a manufacturer's best interest to understand the causes of surface defects. Surface roughness has been shown repeatedly to vary with the build parameters, including laser power, laser speed, hatch spacing, and use of skywriting, as well as differences between the bulk and contour parameters [1, 2, 3]. Other factors, such as the angle of a non-vertical component, have also been demonstrated to affect surface quality [4, 5]. Even the process of converting from computer-aided design (CAD) model, to .stl file, to sliced model, as well as the stair-step effect, can cause errors that are compounded due to the layer-by-layer nature of AM part production [6].

With the goal of minimizing surface roughness, past tests have varied individual parameters in controlled experiments to take samples of roughness data, and some correlate this data to the resulting fatigue life of the component [1, 7]. It has been observed that a set of parameters that is ideal for eliminating surface roughness may result in increased porosity, and vice versa [8]. However, it is believed that small amounts of porosity usually do not have a significant impact on a part's fatigue life, as life is typically dominated by the surface quality [9]. Therefore, it is necessary to understand the specific causes of surface roughness and how to quantify the surface quality in order to make the most accurate life predictions possible.

One AM study made test samples out of aluminum and titanium alloys to mimic hydraulic parts with internal channels. The samples were then cut, and the inside surfaces were measured for Ra (line average roughness), Rz (line maximum height range), and Rp (line highest peak). It was found that these metrics were dependent on the processing parameters as well as the orientation of the part [10]. Another study investigated the effect of speed and laser power on the presence of satellites, balling, holes, and pores on aluminum alloy surfaces. It was found that there exists a range of optimal laser powers, and powers outside of this range create greater amounts of surface defects [11]. A study considering various angled surfaces also found optimal points for speed and power, but these ideal values changed for different build angles. The downskin surfaces showed a decrease in roughness with decreasing power and increasing speed. These trends, however, were reversed for nearly-vertical surfaces [4].

Surface roughness and its relation to mechanical performance have been investigated for traditionally manufactured surfaces. These typically display more predictable performance because of the consistent groove patterns created by the machining device, even though random roughness also exists [12]. One previous study used notched tensile bars and found that triangular notches failed sooner than comparably sized elliptical ones, suggesting that pit depth is not the only determining factor for which defect will be the ultimate cause of failure [13]. In a study on the effect of corrosion on fatigue performance, the depth, surface area, diameter, and volume of the pits were measured, but it was determined that slope, local pit concentration, and relative pit depth were better indicators of where crack initiation would occur [14]. A study in composite materials proposed using Ra to approximate notch depth, combining this value with the notch tip radius and the ratio of the average valley to the maximum one to quantify surface quality [15]. It is clear that while surface roughness is known to contribute to fatigue failure, the AM industry is still lacking in methods of accurately characterizing it and predicting its effect on fatigue performance.

Methods

Coupon Geometries

Specimens were manufactured in two shapes to study the causes of surface roughness in Inconel alloy 718. First, three cubes were made to observe the four vertical 90° surfaces. The sides of the cubes were all 0.5 inches in length and height. Special note was taken of the orientation of the sides with respect to the travel direction of the recoater and air supply. Observing the sides of the cubes means the build parameters of interest are the contour parameters, so the bulk parameters were held constant throughout the build. A top-down diagram of the cube geometry is shown in

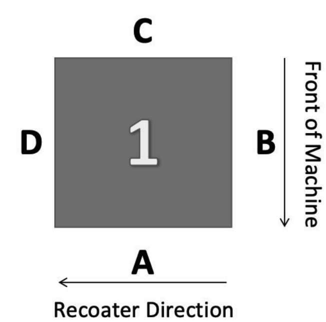

Figure 1: Cube test geometry

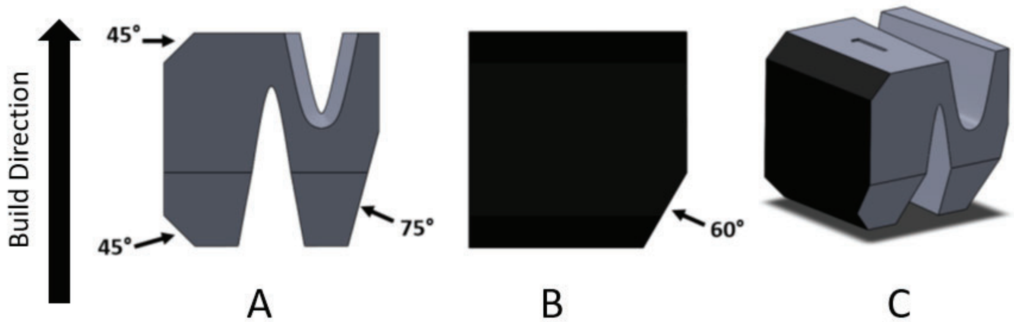

Figure 2: Test Coupon Design in CAD (Front (A), Side (B), and Isometric View (C))

Figure 1. Additionally, custom test coupons, as shown in Figure 2, were designed to observe the effect of specific downskin angles on roughness metrics. The 60° surface will be considered in this parameter study. Angled surfaces tend to be rougher than vertical surfaces, and thus they are of special interest for the purpose of fatigue life prediction. All components were constructed during a single build to limit the effects of external variables.

Additive Manufacturing Processing Parameters

All geometries were fabricated using nickel-based superalloy 718 in an EOS M290 LPBF machine. The parts were built in the layout shown in Figure 3 at a layer thickness of 40 µm. The numbered specimens show the 4 cubes and the 9 test coupons that were fabricated. All the cubes and 6 test coupons are analyzed in this paper. Additional specimens were built at the same time for use in a different study. For all specimens, the bulk parameters were held at the EOS standard parameters for alloy 718.

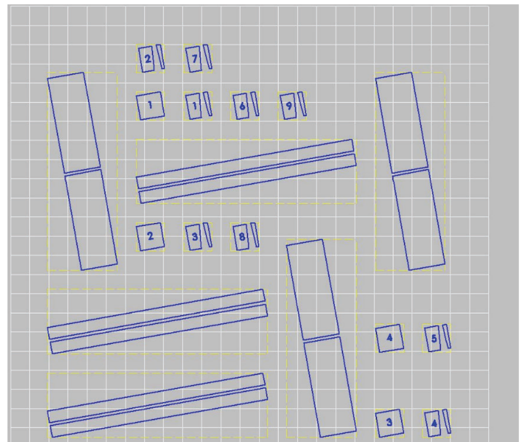

Figure 3: Build platform layout

Cubes Processing Parameters

The parameter sets that are modified to control the vertical surface features are the contour scanning parameters. The contour scanning traces the outside of the part on each 2D layer and the contour parameters are known to relate to the surface roughness on vertical surfaces [1]. Three different contour settings are used in varying the laser power of the contour. The contour laser power (P) is varied (80, 100, 120 Watts) while the speed (S) is held constant (560 mm/sec).

Test Coupon Processing Parameters

The test coupons were designed to look at downward facing surfaces. These surfaces use a different parameter set called a downskin. A downskin parameter is used on an overhanging surface where different parameters are needed to melt the powder particles, because on an overhanging surface the powder is being melted over the loose powder bed rather than solid material within the bulk of the part. Downskin parameters are necessary considering the fundamental heat transfer problem is different than when the material is being melted over solid material. The melting and solidification behavior changes at downward facing surfaces due to the lack of solid material under these surfaces and being supported by the loose powder bed during the process. A downskin parameter is applied by the machine looking at the 2 previous layers of the build to see when it is building over the powder bed.

The downskin parameters were varied where the laser power is P = 75, 95, and 115 Watts with a constant speed of 785 mm/sec and the speed is S = 715, 750, and 785 mm/s with a constant power of 95 Watts. The downskin hatch spacing used was 0.1 mm for all cases. A duplicate test coupon was fabricated at the parameter set P = 95 Watts and S = 785 mm/s. Downskin contour parameters remained constant for coupons examined with a power of 35 Watts and a speed 2000 mm/s. All other machine parameters remained at the manufacturer's recommended settings.

Surface Characterization

Surface scans were conducted using a Keyence VR-3200 light macroscope, which functions by aiming a pair of lights on the specimen's surface and then re-capturing the light using a centralized lens to determine a given point's vertical position. The lens auto-focuses to maintain the highest level of accuracy throughout the scan. Many high-resolution contour maps were produced and then stitched together using the built-in software. A correction factor was applied to each stitched image to account for any angled bias of the measurement surface or bottoms of the samples. The raw height data was then exported as .csv files for statistical analysis.

Surface Roughness Metrics

Surface metrics are used to quantify the characteristics of an AM surface. A prefix of "R" is referring to a line measurement and "S" is referring to a surface metric. For this research, surface measurements were used due to their ability to capture a larger sample size than a line measurement, which has the potential to miss the life limiting surface feature due to its reduced coverage of the surface. Line measurements are also easily affected by outlying features such as a large powder particle stuck to the surface.

The following metrics for surface roughness will be discussed: average roughness (Sa/Ra), root mean square roughness (Sq/Rq), maximum valley (Sv/Rv), maximum peak (Sp/Rp), maximum height range (Sz/Rz), skewness (Ssk/Rsk), and kurtosis (Sku/Rku). These metrics are defined and parameterized in ISO 25178, and equations for calculating these metrics can be found in this same standard [16]. Average roughness is the average difference of all heights relative the mean height of the surface. Root mean square roughness is the square root of the sum of squares of the heights relative to mean height. The maximum valley is the depth of the lowest point relative to the mean height. The maximum peak is the height of the highest point relative to the mean height. The maximum height range is the distance in the direction normal to the surface between the deepest valley and the highest peak. This is equal to the sum of the maximum valley and the maximum peak. Skewness is derived from the probability density curve of the height data of the surface. If the peak of maximum probability does not lie at the mean height, the shift is characterized by the skewness. Kurtosis is also derived from the probability density curve. The sharpness or rate of rise of the probability peak is quantified by the surface's kurtosis value.

Results

Each height data set was imported into MATLAB. The entire surface was measured but obtaining a single metric for the whole surface may not be precise enough to sufficiently describe the surface. Therefore, 16 regions were used in a 4x4 arrangement. The surface roughness metrics were calculated for every region individually. The averages and standard deviations were calculated and are reported in the following sections and related to their corresponding processing parameters.

Influence of Contour Processing Parameters on 90° Surface Roughness

The calculated surface metrics of the vertical cube surfaces are displayed in Figure 4 with error bars representing one standard deviation in each direction. Some metrics are more closely correlated to the fatigue performance of the part than others. Specifically, Sv, which represents the maximum notch depth below the average surface height, has been identified as a useful indicator of fatigue life [1]. However, since this value is gauged from the average surface location, Sa and Sp are necessary references that are key to fully understanding Sv. The 80 W cube specimen was found to have noticeably lower Sp values than the other power settings. Although Sp seems to be largely unrelated to fatigue life, having a small Sp value can lower the respective Sa value. This means that the maximum notch depth is being measured from a lower benchmark, causing the resultant Sv to appear less harmful than it might actually be.

If the 80 W Sv is considered understated, a trend of decreasing Sv with increasing power becomes apparent. This result supports the findings by Gockel et al., who used similar speed and power parameters to find the same trend [1]. No clear trends are visible for skew and Sp, but the data does indicate an increase in kurtosis with increasing power. A high kurtosis value indicates that the distributions of heights has a close proximity to the mean. This further emphasizes that increasing the power setting creates fewer extreme outliers in the form of either peaks or notches.

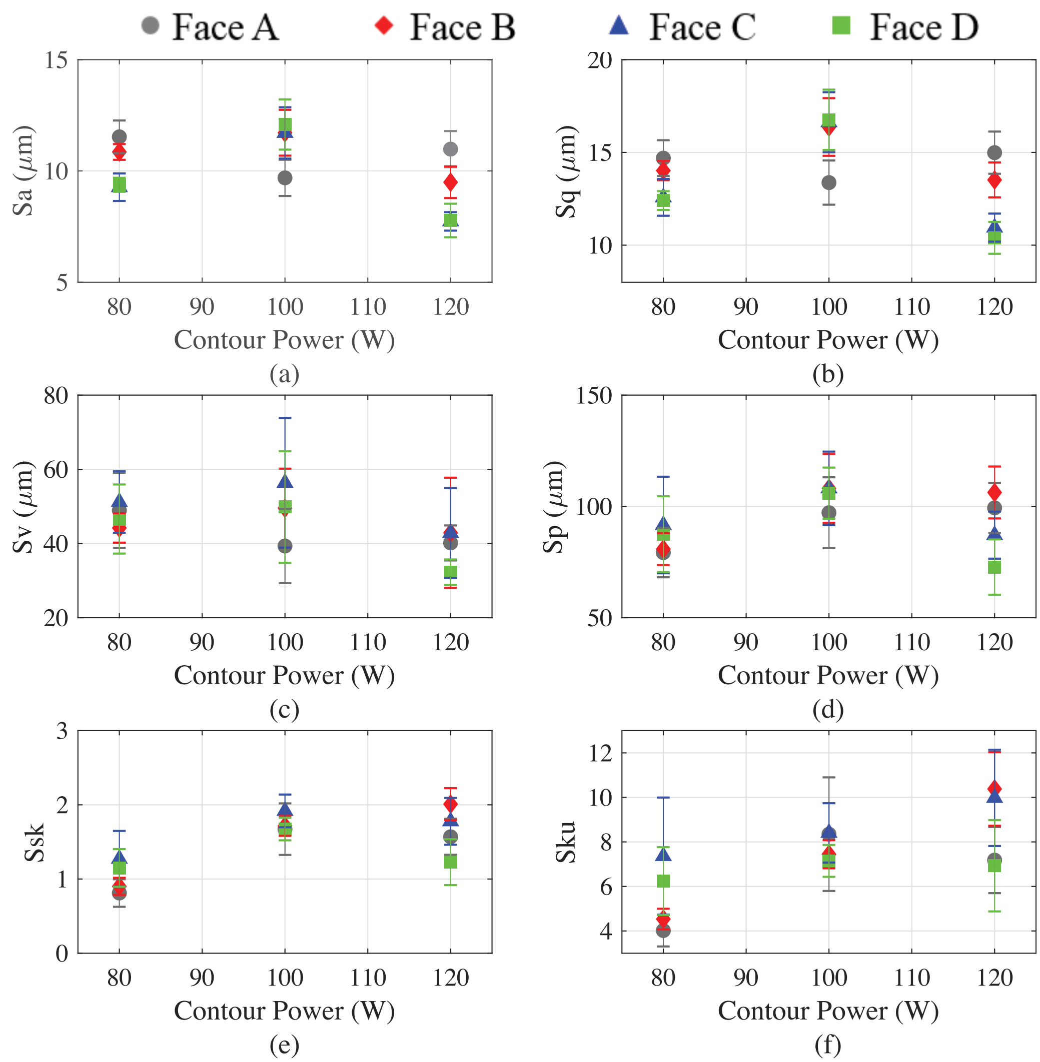

Figure 4: The influence of contour laser power on surface roughness metrics

Visual Comparison of Surfaces at Different Downward Facing Angles

The roughness of the surfaces increases in severity as the downward facing angle goes from 75°, to 60°, and to 45°. This can also be noticed when visually looking at the roughness, as seen in Figure 5. With the same scalebar used for on the height plot there is less red (high peaks) and blue (deep valleys) in the 75° surface compared to the 60° and 45° surfaces. This trend was expected because as the angle goes from 75° to 45° the amount of the surface that is being melted on top of the loose powder bed and not the solid previous layer increases.

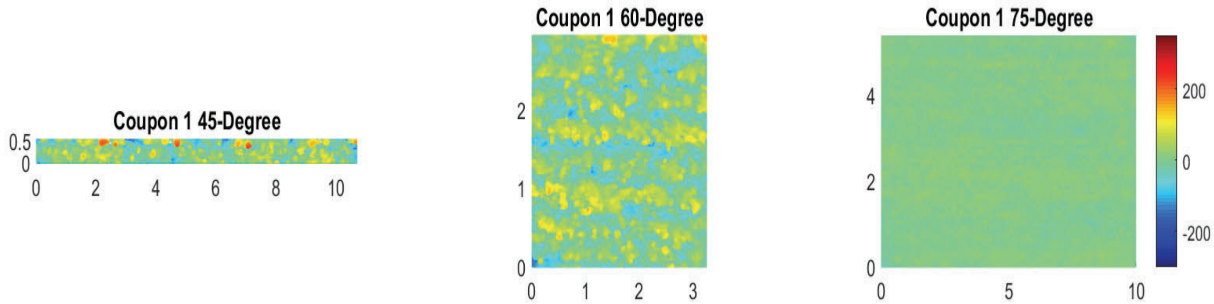

Figure 5: Comparison of surface roughness plots at different downward facing angles. Heights measured in µm, surface dimensions in mm. All heights are of equal scale.

Influence of Downskin Processing Parameters on 60° Surface Roughness

To further understand the downward surfaces, surface scan measurements were taken of the 60° surfaces. Plots relating the processing parameters (speed and power) to the surface roughness metrics were made to observe the trends about the influence of parameters for the 60° downward facing angles. The results of these measurements are discussed in the sections below.

In addition, when observing the height data of the 60° surface, a periodic behavior can be seen in all the test coupons potentially caused by thermal and layering effects during build. These effects could be caused by the powder recoater spreading fresh powder as the build plate lowers to complete the build layer by layer. The peaks and valleys seem to alternate as the build was completed, as seen in Figure 6.

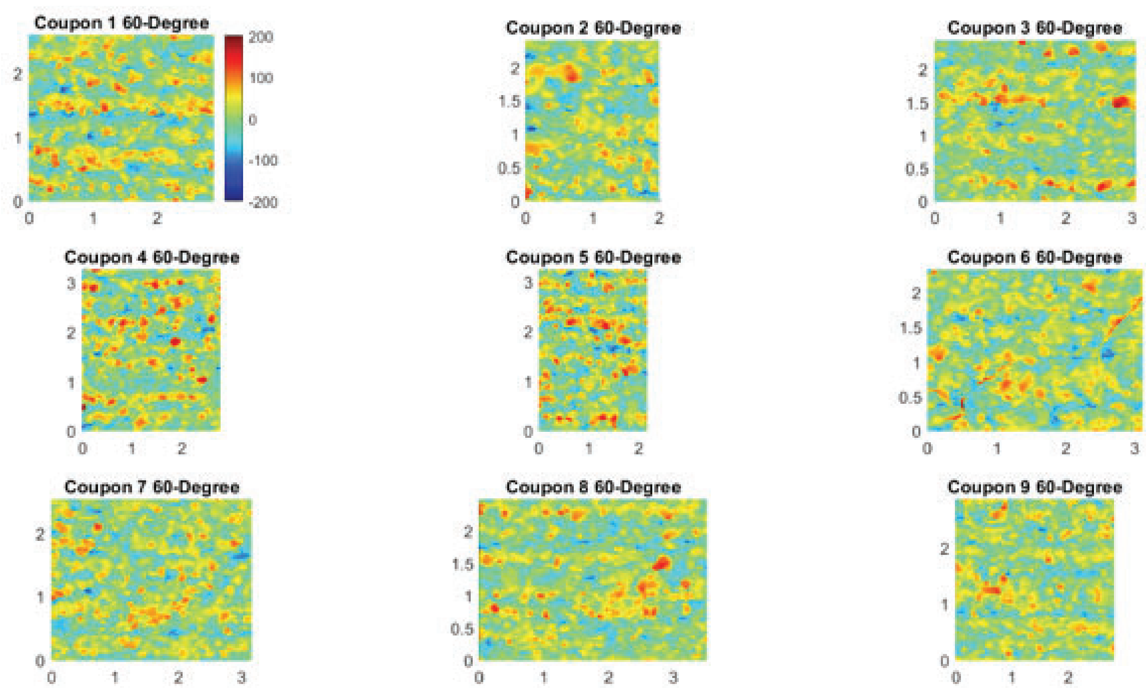

Figure 6: Periodic Behavior in the 60° Test Coupon. Heights measured in µm, surface in mm. All heights are of equal scale.

Effect of Downskin Laser Power

This section describes the influence of changing the downskin power on the surface roughness metrics for a 60° surface as shown in Figure 7. The downskin speed is held at a constant value of 785 mm/s. The measurement metrics applied were gathered using the same methods as with the cubes, and the standard deviations are once again shown as error bars. For these plots, it can be noticed that there is a replicate test coupon made at 95 Watts, and 785 mm/s. These values should agree closely since they are the same parameter set. However, in some of the plots below one will notice significant differences between these two values. This could be due to the locations of the specimens on the build plate, or statistical variance.

As the power increases there is a decrease in the mean surface roughness. This trend is also seen in the literature. However, for this work different processing parameters and downward angle was used but results are still following the same trend. As the power increases, the maximum valley depth is shown to decrease. The max peak height and the maximum peak to valley versus the downskin power do not shown any significant trends. The skewness and the kurtosis do not show significant differences in the results.

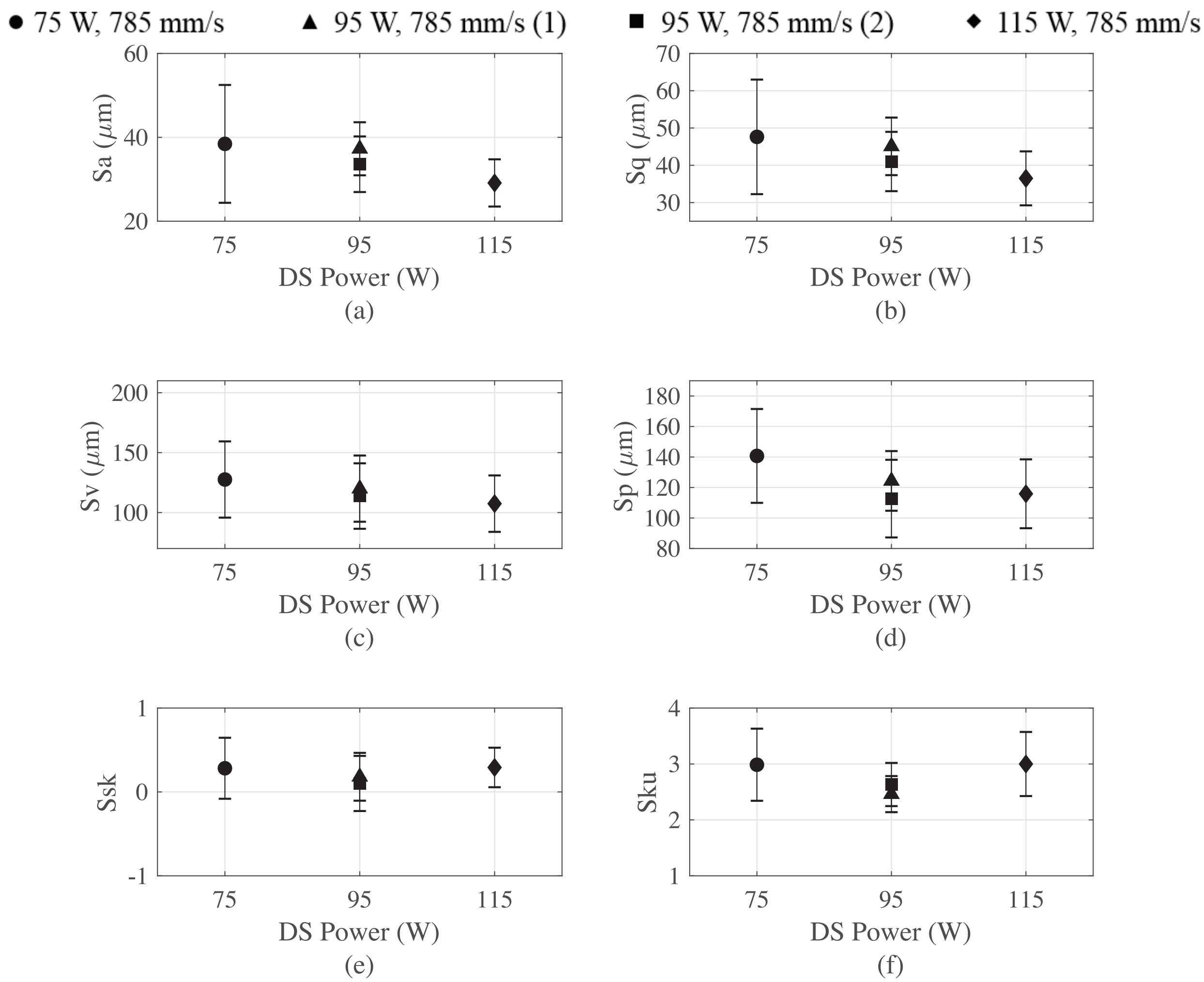

Figure 7: Downskin surface roughness parameters (a) Average roughness (Sa), (b) Root mean squared roughness (Sq), (c) Maximum notch (Sv), (d) Maximum Peak (Sp), (e) Skewness (Ssk), and (f) Kurtosis (Sku) with respect to laser power

Effect of Downskin Laser Speed

This section describes the influence of changing the downskin speed on the surface roughness metrics for the 60° surfaces as shown in Figure 8 with standard deviations. The downskin power is held at a constant value of 75 W. As the speed increases there is a slight increase in the Sa values, however this difference is very small and likely to be negligible. In previous work on vertical surfaces, the average Sa value was between 8 and 14 µm [17]. For the 60° surface, the average Sa values are much higher at approximately 40 µm. This shows the importance of understanding the angle of the downward surfaces to improve average roughness values. As the speed increases the maximum valley decreases and the maximum peak height increases. These max peaks are likely caused by powder particles stuck to the fully melted surface. As the speed increases the skewness increases and the kurtosis also increases.

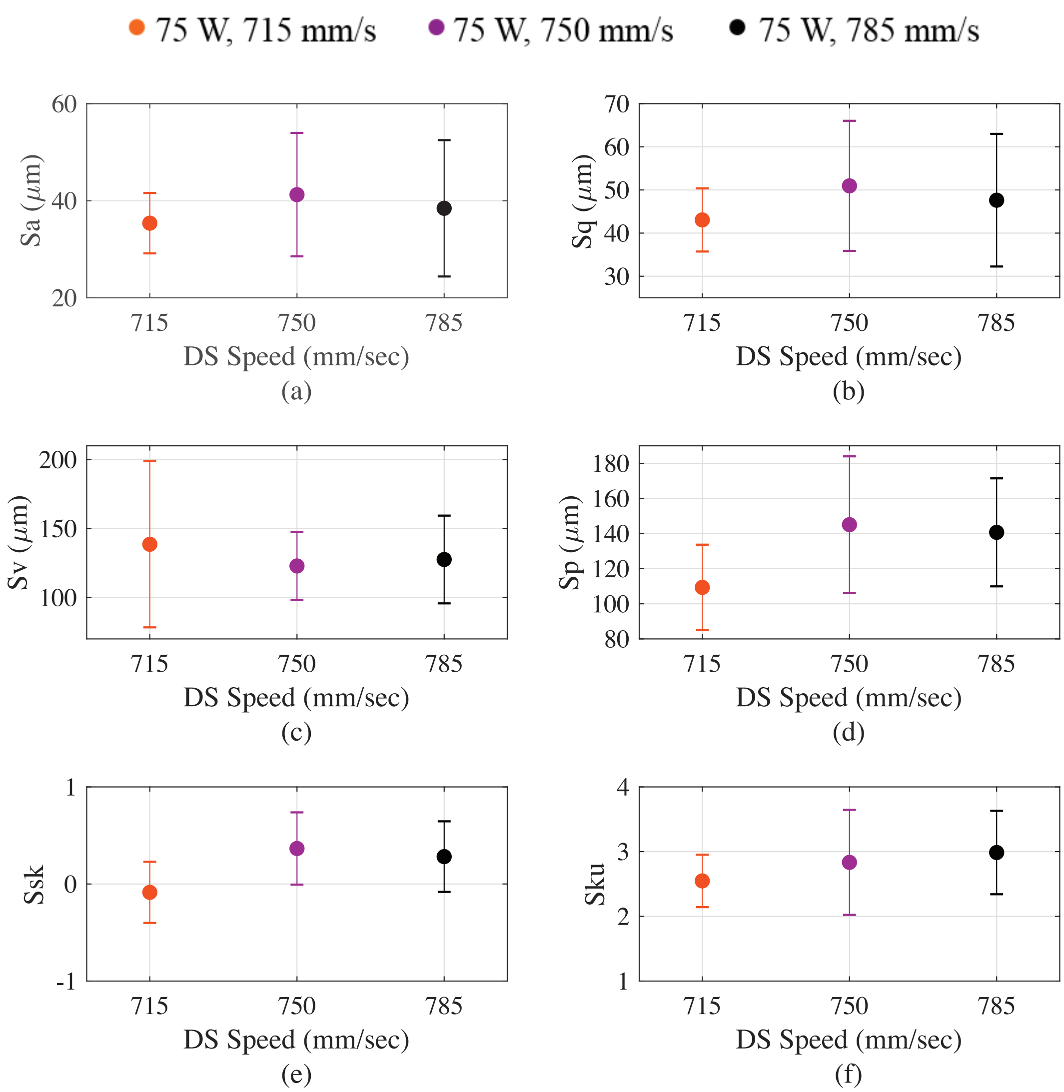

Figure 8: Downskin surface roughness parameters (a) Average roughness (Sa), (b) Root mean squared roughness (Sq), (c) Maximum notch (Sv), (d) Maximum Peak (Sp), (e) Skewness (Ssk), and (f) Kurtosis (Sku) with respect to laser speed

Discussion

Surface Roughness Maximum Valley Variation

A significant portion of the data points in Figure 4, Figure 7, and Figure 8 lie within the standard deviations of the other parameters. This demonstrates the volatility inherent to the additive process, since individual surfaces can have regions with such varying degrees of roughness. Increasing the sample size by considering the individual faces separately allows for an increase in confidence in the trends observed, but in some cases, this also increases the spread. Many more build analyses will be necessary to achieve high confidence in the trends, but even then, results are likely to see some variation from additive machine to additive machine and from build to build. Some causes and consequences of these variations are discussed in later sections.

The surface roughness can also be represented in a line form denoted by R instead of S. The maximum valley parameter is therefore Rv. The line metrics can be calculated from the structured light scanning method. The Rv values for the cube geometry were calculated parallel to the build direction along each surface. The structured light scanning method produces a matrix of height data with the columns parallel to the build direction and the rows perpendicular to the build direction. Rv was calculated for each column of the cube height data. First a column is extracted, then the data is centered to where the mean is zero. The maximum valley in the centered data is taken to be Rv. This value is calculated for all columns of the data and the Rv in each column is plotted in Figure 9. Rv varies dramatically depending on where the line measurement is taken. There are several locations where uncharacteristically large valleys are measured.

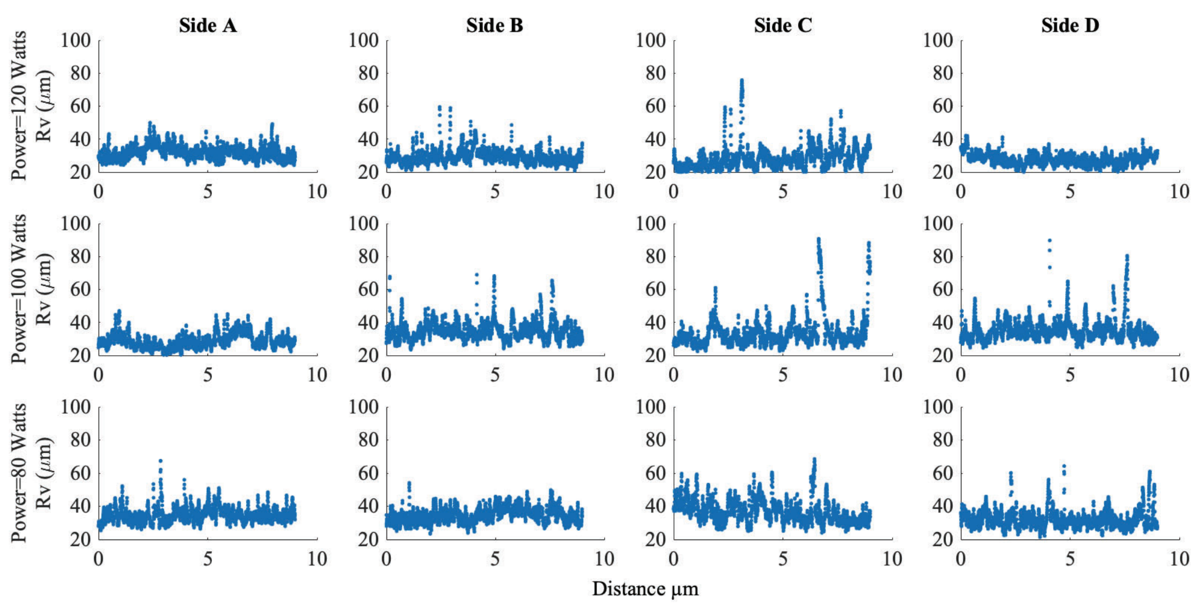

Figure 9: Maximum valley (Rv) calculated for each line parallel to the build direction (mm)

If all Rv values for each side are averaged, the values are plotted in Figure 10. As the contour power is increased, the surface roughness decreases. However, when the maximum Rv that is measured from each side is plotted, the trends are not as apparent. It is not immediately apparent if the depth of the maximum valley on a surface is correlated to the average line measurement Rv. However, fatigue performance is often dictated by the maximum defect. Therefore, it cannot be confidently said that taking one, or even a handful, of line measurements will allow for accurate prediction of a specimen's fatigue life. Even if they are not identified, the maximum valleys would still be a concern for mechanical performance such as fatigue behavior.

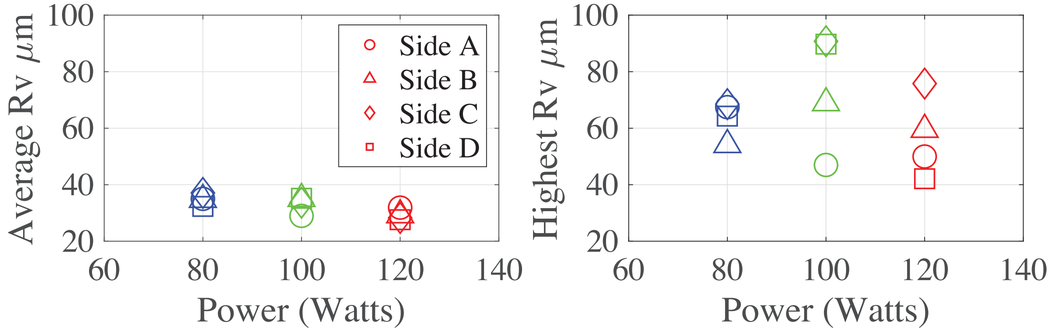

Figure 10: Maximum valley line measurement for each sample (a) average and (b) overall max values.

Valley Finding

In order to investigate the valleys on the surface, a method was developed and implemented to find and record valleys in the surface. This is demonstrated using the cube specimens. The applied method is called the comparative value method in this work. The comparative value method uses logical operators to compare data points with their neighbors. If the data point has a lower surface height than its neighbors for a certain number of surrounding rings within the height matrix, it is recorded as a valley. The global depth relative to the mean surface and indexes of the valley is then recorded in the valley matrix, which is used to plot and analyze these valleys. The method includes 8 points per ring and the user defines the number of rings. Valley data for 15, 23, and 50 ring comparisons are shown in Figure 11.

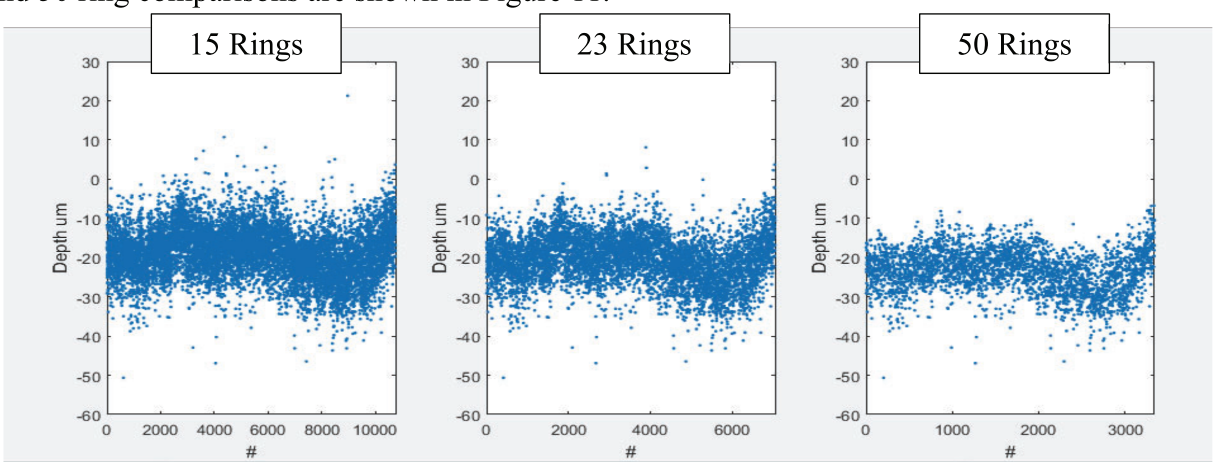

Figure 11: The depths of valleys found using (a) 15 rings, (b) 23 rings and (c) 50 rings

As the number of rings examined increases, the average depth appears to be shifting down and fewer valleys are identified. As the comparison area is expanded, some of the smaller valleys will not be detected because of proximity to larger ones. In an area defined by a square whose corners are 50 points away from the center, more than one valley could exist. Therefore, any valley within 50 points of another valley might not be detected. Using a large search area will inherently decrease accuracy once it becomes larger than average valley sizes. The very deepest valleys will likely still be revealed; however, while the depth of the valleys is an important parameter, other characteristics of the valleys are likely to be important as well when considering the impact on mechanical performance. Sharp cracks, as well as long ones, may be lost if they are shadowed by a slightly deeper neighboring valley. In all, using fewer rings is the safer but more intensive method that should be used when practical.

Measurement Challenges

In addition to using the Keyence to characterize the test coupon surfaces, a scanning electron microscope (SEM) was used to further investigate the surfaces. A visual surface irregular peak that showed up in the height data was caused by “fiber” on the surface as shown in Figure 12. This fiber remained on the sample after treating the sample with compressed air before placing it in the SEM for observation as shown in Figure 13. This small detail could make a significant difference in average surface metric values. This fiber would not influence material performance, yet it registered on the surface scan as the highest peaks, skewing the measurements. This shows how a small detail such as a fiber is capable of altering even meticulously taken surface measurements.

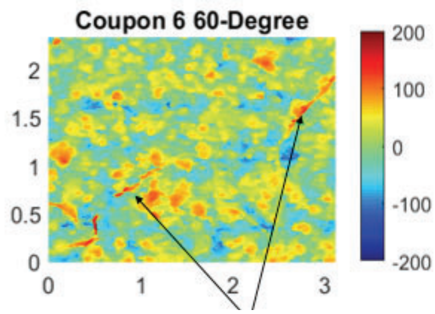

Figure 12: Surface scan showing highest roughness peak (μm) represented by the fiber stuck to the surface (mm)

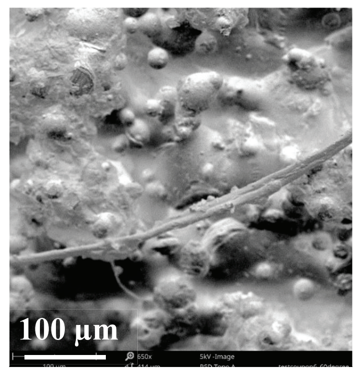

Figure 13: SEM image showing fiber stuck to the surface

Conclusions

This work explored the influence of processing parameters on the surface roughness in laser powder bed fusion additive manufacturing. Vertical surfaces are controlled by the contouring parameters, and it was found that increasing the contour laser power decreased the surface roughness. For a downward facing surface, there are downskin parameters that influence the formation of the surface. A similar trend was seen in that increasing the laser power of the downskin parameter created a less rough surface.

The variation in the notches on the surface was investigated. A line measurement of the maximum notches showed that parameters can be used to control the average valleys of the notches, however, the maximum values do not display significant trends with parameters. Additionally, it has been observed that compromises must be made when identifying valleys, and that threatening cracks can be overlooked when using only a single metric to categorize defects.

References

[1] J. Gockel, L. Sheridan, B. Koerper and B. Whip, "The influence of additive manufacturing processing parameters on surface roughness and fatigue life," *International Journal of Fatigue,* vol. 124, pp. 380-388, 2019.

[2] M. Xia, D. Gu, G. Yu, D. Dai, H. Chen and Q. Shi, "Influence of hatch spacing on heat and mass transfer, thermodynamics and laser processability during additive manufacturing of Inconel 718 alloy," *International Journal of Machine Tools & Manufacture,* vol. 109, pp. 147-157, 2016.

[3] D. Watring, K. C. Carter, D. Crouse, B. Raeymaekers and A. D. Spear, "Mechanisms driving high-cycle fatigue life of as-built inconel 718 processed by laser powder bed fusion," *Material Science and Engineering A,* vol. 761, 2019.

[4] Y. Tian, D. Tomus, P. Rometsh and X. Wu, "Influeunces of Processing Parameters on Surface Roughness of Hastelloy X Produced by Selective Laser Melting," *Additive Manufacturing,* no. 13, pp. 103-112, 2106.

[5] J. Fox, F. Kim, Z. Reese, C. Evans and J. S. Taylor, "Investigation of complementary use of optical metrology and x-ray computed tomography for surface finish in laser powder bed fusion additive manufacturing," in *European Society for Precision Engineering and Technology Special Interest Group*, 2017.

[6] G. Strano, L. Hao, R. Everson and K. E. Evans, "Surface roughness analysis, modelling and prediction in selective laser melting," *Journal of Materials Processing Technology,* vol. 213, no. 4, pp. 589-597, 2013.

[7] R. Shrestha, J. Simsiriwong and N. Shamsaei, "Fatigue behavior of additive manufactured 316L stainless steel parts: Effects of layer orientation and surface roughness," *Additive Manufacturing,* vol. 28, no. 23-38, 2019.

[8] J. A. Cherry, H. M. Davies, S. Mehmood, N. P. Lavery, S. G. R. Brown and J. Sienz, "Investigation into the effect of process parameters on microstructural and physical properties of 316L stainless steel parts by selective laser melting," *The International Journal of Advanced Manufacturing Technology,* vol. 76, pp. 869-879, 2015.

[9] D. Greitemeier, C. Dalle Donne, F. Syassen, J. Eufinger and T. Melz, "Effect of surface roughness on fatigue performance of additive manufactured Ti-6Al-4V," *Materials Science and Technology,* vol. 32, no. 7, pp. 629-634, 2016.

[10] J. Pakkanen, F. Calignano, F. Trevisan, M. Lorusso, E. P. Ambrosio, D. Manfredi and P. Fino, "Study of Internal Channel Surface Roughnesses Manufactured by Selective Laser Melting in Aluminum and Titanium Alloys," *Metallurgical and Materials Transactions,* vol. 47A, pp. 3837-3844, 2016.

[11] T. Yang, T. Liu, W. Liao, E. MacDonald, H. Wei, X. Chen and L. Jiang, "The influence of process parameters on vertical surface roughness of the AlSi10Mg parts fabricated by selective laser melting," *Journal of Materials Processing Tech.,* no. 266, pp. 26-36, 2019.

[12] E. Hess, The CNC Cookbook: An Introduction to the Creation and Operation of Computer Controlled Mills, Router Tables, Lathes, and More, Scited Publications, 2009.

[13] J. Chen, B. Diao, J. He, S. Pang and X. Guan, "Equivalent surface defect model for fatigue life prediction of steel," *International Journal of Fatigue,* no. 110, pp. 153-161, 2018.

[14] N. E. Co and J. T. Burns, "Effects of macro-scale corrosion damage feature on fatigue crack initiation and fatigue behavior," *Internation Journal of Fatigue,* no. 103, pp. 234-247, 2017.

[15] M. D. Arola, "An Examination of the Effects from Surface Texture on the Strength of Fiber Reinforced Plastics," *Journal of Composite Materials,* vol. 33, pp. 102-123, 1999.

[16] *ISO 25178-2, Geometrical product specifications (GPS)- Surface texture: Areal- Part 2: Terms, definitions and surface texture parameters,* 2012.

[17] B. Whip, L. Sheridan and J. Gockel, "The Effect of Primary Processing Parameters on Surface Roughness in Laser Powder Bed Additive Manufacturing," *The International Jounral of Advanced Manufacturing Technology,* 2019.